

6. M. Skeldon and R. Bahr, to be published in *Optics Letters*.
7. W. Kaiser and M. Maier, in *Laser Handbook*, edited by F. T. Arecchi and E. O. Schulz-Dubois (North-Holland Publishing Co., Amsterdam, 1972), Vol. 2, Chap. E2, pp. 1078-1150.
8. K. S. Jammu, G. E. St. John, and H. L. Welsh, *Can. J. Phys.* **44**, 797 (1966).

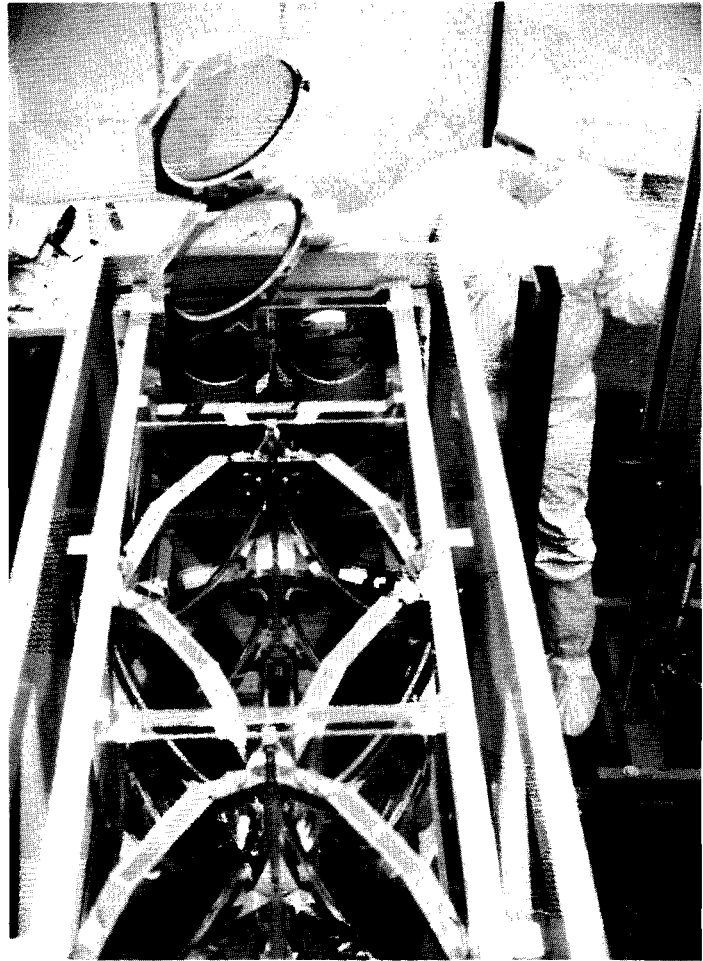
## 1.C Energy Transport Measurements in a Multisegmented Amplifier (MSA)

During the last quarter of 1989 final assembly and checkout were performed on the 24-cm-aperture multisegmented amplifier (MSA). The MSA in final assembly is shown in Fig. 44.11. The amplifier consists of two pairs of disk amplifiers, each five disks deep, that share a common central flash-lamp array. The MSA configuration reduces the ratio of reflector material to Nd:glass. Since flash lamps reabsorb and re-emit their own light with less than unity efficiency and reflectors are never perfect, the MSA central array is expected to be more efficient at pumping the disks, thereby raising the amplifier storage efficiency. This is highly desirable for long-pulse laser systems, where system efficiency is of paramount interest and the appropriate figure of merit is dollars-per-focusable joule.

During the course of this work, the importance of power balance on target became known.<sup>1</sup> While the MSA architecture is eminently suitable for a multimegajoule fusion laser facility<sup>2</sup> (such as the NOVA Upgrade) where one MSA amplifies one beam consisting of up to 16 beamlets, in the OMEGA Upgrade one MSA would amplify four independent beams. Because each of these beams requires independent gain adjustability to obtain power balance, which is difficult with the MSA, the decision was made to use single-beam amplifiers in the OMEGA Upgrade. Therefore, the MSA was completed as an important contribution to the NOVA Upgrade and the technology used as a first step in the development of disk amplifiers for the OMEGA Upgrade. Here we report on the energy-transport measurements made on the MSA during the first and second quarters of 1990.

### Amplifier Description

The MSA is shown in more detail in Fig. 44.12. The individual 3.3-cm-thick phosphate-glass disks have a 24-cm clear aperture. This is 4 cm larger than necessary for a single beam since the amplifier is designed to be angularly double passed as shown in Fig. 44.13. The angle between the entering and exiting beams is 20 mrad. All testing of the amplifier was performed in this configuration. The disks were elliptically masked presenting a circular aperture to the beams in order to avoid pumping unused glass.



G2878

Fig. 44.11

The MSA amplifier under assembly in a class-100 clean room. A pair of disks in their frame is being lowered into the amplifier. The four apertures are visible at the top of the amplifier frame. Some of the five disks for each beam are visible in the foreground.

The amplifier contains 160  $N_2$ -cooled, 1.9-cm bore Xenon flash lamps with a 58-cm arc length. The lamps are oriented vertically to avoid interference with the disk ends thereby permitting closer packing of the lamps to the disks. There are 80 lamps in the interior array positioned on 1-in. centers and 40 lamps in each of the exterior arrays positioned on 2-in. centers. There are no reflectors between the lamps in the interior array. The lamp-packing fraction is 1.175. Each lamp in the interior array is wrapped with a grounded Nichrome wire to enhance triggering. Blast windows of a water-white float glass 0.25 in. thick are mounted on both sides of the interior arrays and on one side of the exterior arrays. Reflectors are used on only the exterior arrays and are simple searchlight reflectors, the center of each lamp located at one-half of the radius of its individual reflector cusp. The reflectors are dip-coated silver, >95% reflecting over the entire pump spectrum, 400–900 nm.

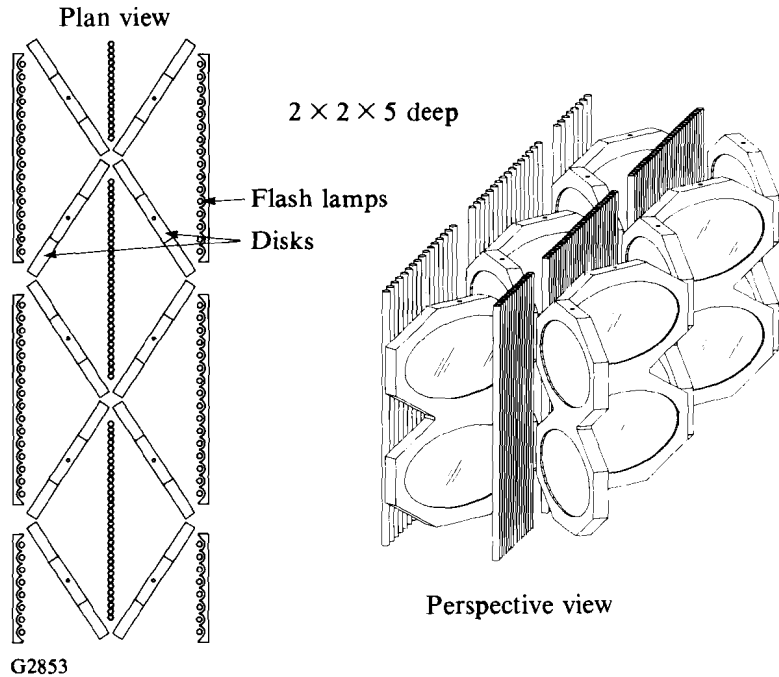


Fig. 44.12

Schematic of the MSA. The top and bottom reflectors and the near-side flash lamps are not shown for clarity. Note that the central flash-lamp array has twice the packing density of the outboard arrays.

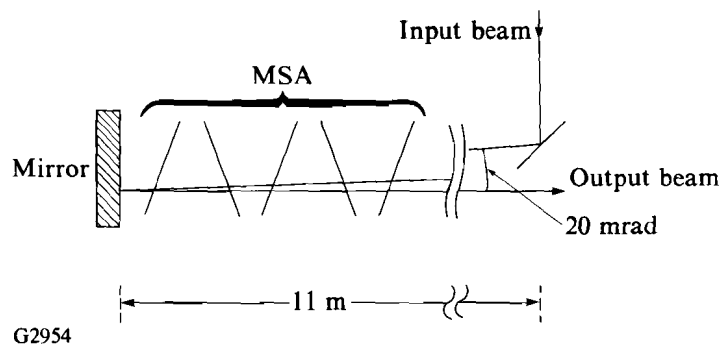


Fig. 44.13

Angular double passing of the MSA. The 11-m propagation distance and the 20-mrad angle between input and output beams allows for a separation of 6.4 cm between beam edges.

Four lamps are connected in series and driven by one pulse forming a network consisting of a  $100\text{-}\mu\text{F}$  capacitor and a  $278\text{-}\mu\text{H}$  inductor. The lamps are also preionized<sup>3</sup> by a weak discharge initiated  $200\ \mu\text{s}$  prior to initiation of the main discharge. The design-charging voltage is 21.5 kV for a total nominal capacitor-bank energy of 924 kJ. This bank energy will be referred to as “100% nominal bank energy” throughout the remainder of this article.

### Experimental

Two sets of energy-transport measurements were made: small- and large-signal gain. These can be self-consistency checked with a Frantz-Nodvik<sup>4</sup> model of the amplifier, coupled with a knowledge of the losses in the amplifier. These measurements were done as a function of percent bank energy. This yielded valuable information on the dynamics of the pumping process.

The small-signal gain was measured with the apparatus shown in Fig. 44.14. This apparatus measures the small-signal gain at three locations in one of the clear apertures. In all of the measurements reported here the small-signal gain was measured in the plane of incidence of the disks (horizontal). The locations were the center of the clear aperture and 1.0 cm from the edge of the clear aperture. A polarized cw Nd:YLF oscillator operating on the 1.054- $\mu\text{m}$  transition is split three ways. Each of the three beams then double passes the amplifier. The return beam is first dispersed with a grating to reduce the spectrally near fluorescence. The beam is then reflected from a 1- $\mu\text{m}$  mirror to limit the amount of flash-lamp light seen by the detector. Each beam is spatially filtered with a 1-mrad cutoff full angle before detection to further limit both fluorescent light and lamp light. Large-area photodiodes with a measured  $1/e$  response time of 2  $\mu\text{s}$  detected the signals. A fourth identical photodiode monitored the Nd:YLF laser output as a reference.

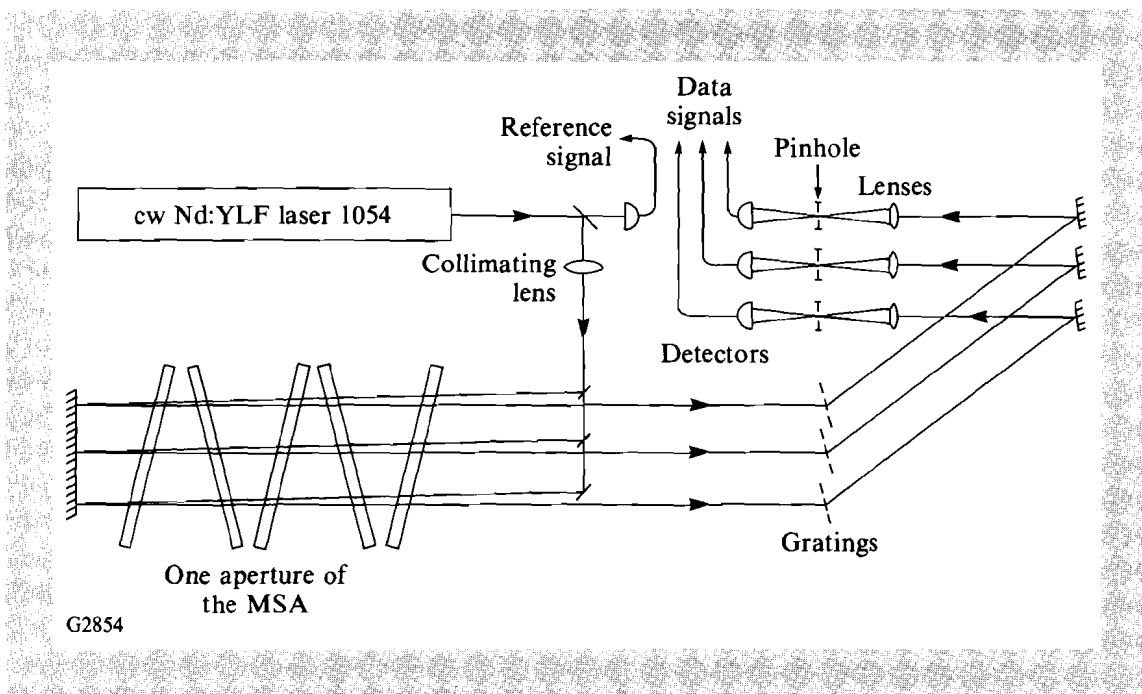


Fig. 44.14  
Schematic of the small-signal-gain measurement apparatus. The cw Nd:YLF laser is split into three beams that probe different locations within the *same* aperture. The return signals are filtered spectrally with gratings and spatially filtered before detection.

Signals from the large-area photodiodes were digitized by Tektronix<sup>5</sup> 2440 oscilloscopes with 500 megasample-per-second maximum-digitizing rate. Signals were digitized into 2-ms, 1024 sample-record lengths with 8-bit amplitude resolution. The 2.0-ms record length ensured that the entire temporal history of the gain and a portion of all signals prior to the initiation of the flash-lamp discharge were recorded. The signals were then Fourier transformed, filtered with a Blackman<sup>6</sup> filter whose cutoff frequency was 100 kHz. A background “shot” was taken for each gain measurement. For the background shot, the cavity of the Nd:YLF was blocked and all of the above signals were recorded. This background included fluorescence from the amplifier and any non-cancelling noise. The background for each channel was subtracted from the data for that channel. The temporal variations of the Nd:YLF were removed by dividing each of the three signal channels by the reference channel. A 200- $\mu$ s sample of each of the three channels prior to initiation of discharge was averaged and set equal to unity. The remainder of the data in that channel was multiplied by the so-determined constant to convert the data to small-signal gain. The estimated precision attained as a result of this procedure is  $\pm 1\%$ . The gain of a reference 90-mm-rod amplifier could be routinely remeasured with this precision.

For the large-signal-gain measurements the amplifier was deployed on the OMEGA laser system as shown in Fig. 44.15. The output of the OMEGA 90-mm-diam rods, after expansion to 160 mm by the output spatial filter, was turned 90° and further expanded to 180 mm by a Galilean expander. The 180-mm beam was turned 90° and double passed the amplifier. The output of the amplifier was spatially filtered in an  $f/14$  spatial filter with a 475- $\mu$ rad full-angle cutoff. The input and output energies were measured calorimetrically.<sup>7</sup> The input energy was taken from an uncoated pickoff prior to the Galilean upcollimator. The output energy was taken from a similar uncoated pickoff after the  $f/14$  output spatial filter.

## Results

The measured small-signal gain at three positions within one aperture of the MSA as a function of percent of nominal bank energy is shown in Fig.

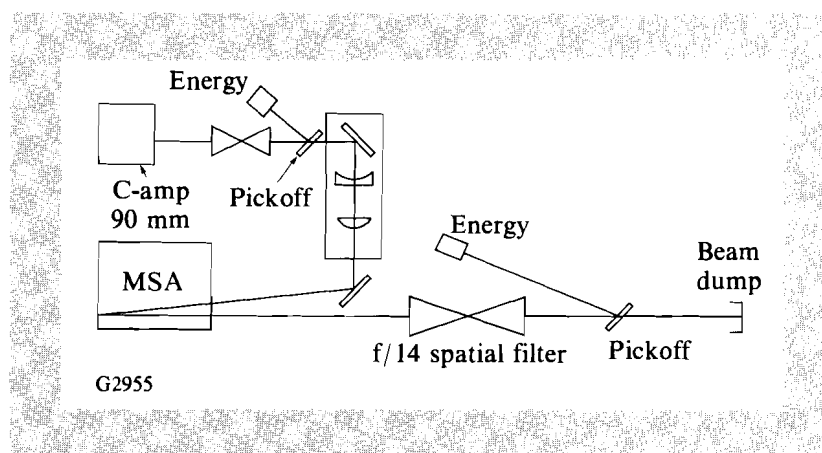


Fig. 44.15  
Schematic of the large-signal-gain experiment. The 90-mm output of beamline 6-2 of the OMEGA laser system was magnified by 2, turned, further magnified by 1.10, and turned into the amplifier. The output of the amplifier was spatially filtered by an  $f/14$  filter with a 475- $\mu$ rad full-angle cutoff.

44.16. The small-signal design goal of 11.8 in double-pass was achieved at ~65% of the nominal bank energy. The center of the aperture consistently displayed the highest gain. The edge of the aperture closest to the interior array was slightly higher in gain than the outboard array, lending support to reports<sup>8</sup> that the interior arrays are more efficient in pumping Nd<sup>3+</sup>. At high percentages of nominal bank energy, the main discharge often initiated before completion of the preionization. This reduced the maximum achieved gain and is in part responsible for the deviation from linearity in Fig. 44.16.

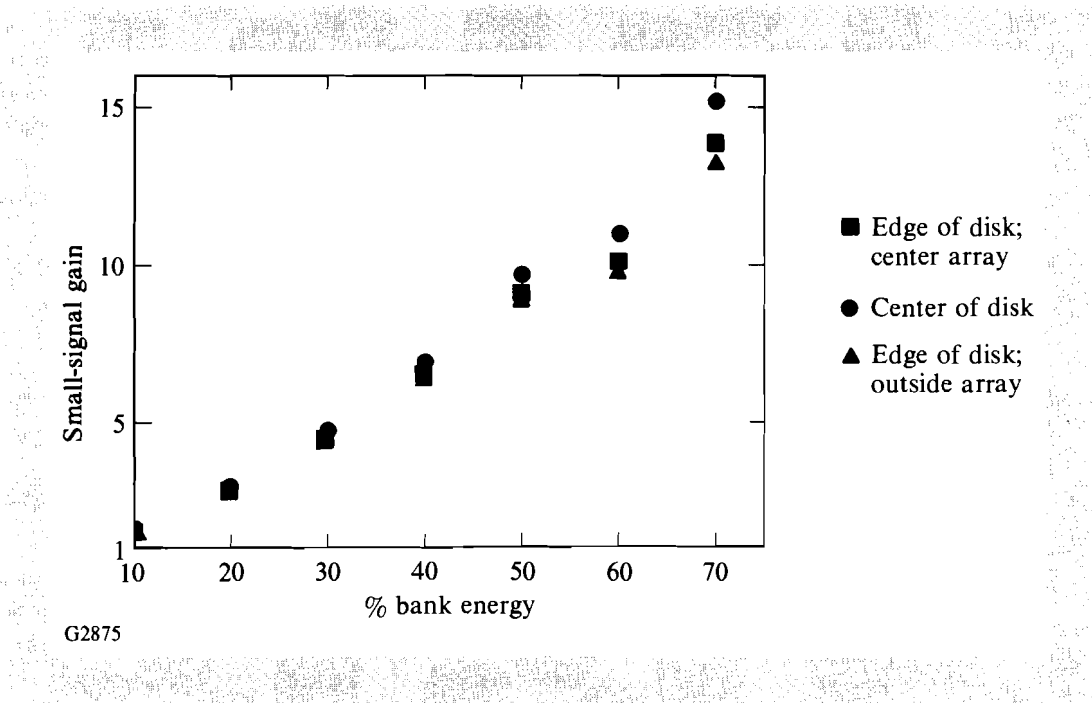
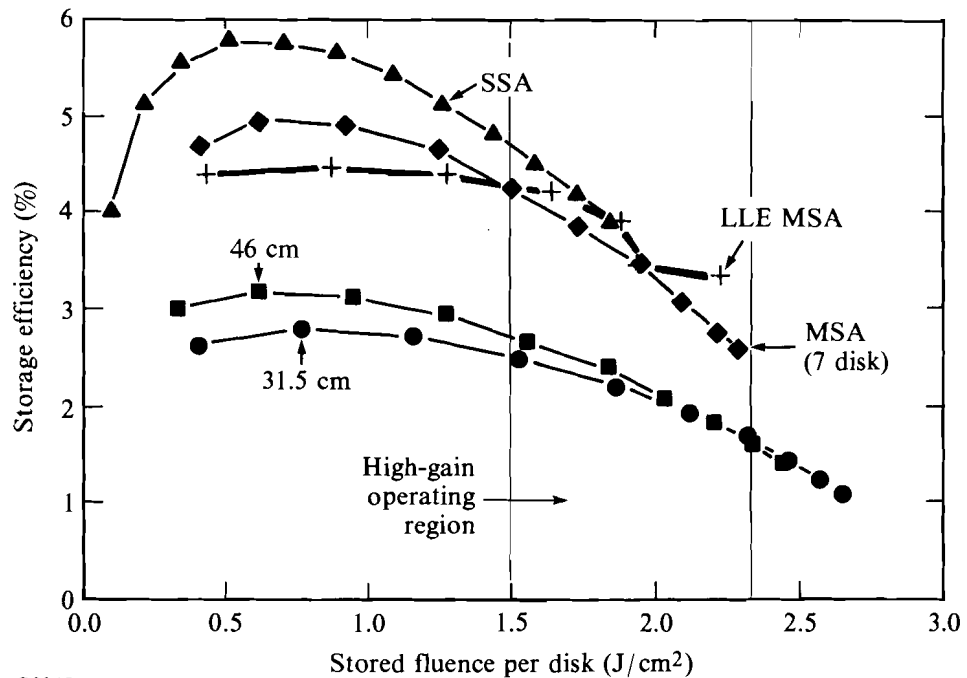


Fig. 44.16 The small-signal gain of the three locations plotted versus percent nominal bank energy. The small-signal design goal of 11.8 was achieved at 65% of the design-bank energy.

The overall storage efficiency, defined as stored energy in the glass divided by the stored energy on the capacitor bank, is shown in Fig. 44.17 plotted versus the stored fluence per disk. The stored fluence per disk is the stored energy-per-unit-beam-area per disk. Also shown on this same plot is the performance of several other disk amplifiers, both standard box design and MSA. All of these plots are based on an assumed stimulated-emission cross section of  $3.5 \times 10^{-20} \text{ cm}^2$ . The plot displays the characteristic high-cavity efficiency at lower lamp loadings due to reduced cavity opacity and declining efficiency as the gain increases, the cavity opacity increases, and amplified spontaneous emission (ASE) begins to become significant. The high cavity-transfer efficiency near the design goal of  $2.06 \text{ J/cm}^2$  ( $0.34 \text{ J/cm}^3$ ) is particularly surprising since this MSA used a



G2845

Fig. 44.17

Disk-amplifier storage efficiencies plotted versus the stored fluence per disk. The stored fluence per disk is the stored energy-per-unit-beam-area per disk. The MSA architecture is very efficient relative to other disk amplifiers in the region of interest around  $2.0 J/cm^2$ .

circular clear aperture instead of a square clear aperture. It is evident that the improved packing and reduced losses of the MSA architecture can result in improved amplifier efficiency.

The large-signal gain of the MSA plotted versus percent nominal bank energy is shown in Fig. 44.18. The drive into the amplifier from the OMEGA laser system was held constant at  $130 \pm 6 J$  for this series. An output of  $950 J$  was achieved at 70% of nominal bank energy. This actually outperformed the design goal of  $1000-J$  output with  $185-J$  drive at 100% of nominal bank energy.

One additional observation not widely reported previously was that for a period of 1 to 2 s following a high bank-energy shot, the amplifier cavity was observed to glow with a bluish color. The glow decayed slowly enough to permit photographing the amplifier using no other light source. It is presently hypothesized that the glow is due to the auroral bands of  $N_2$ .

### Conclusion

The MSA has been demonstrated at full scale as a particularly efficient amplifier. Storage efficiencies in excess of 4% have been achieved with good gain uniformity. These measurements support the choice of the MSA architecture for an LMF-scale facility.

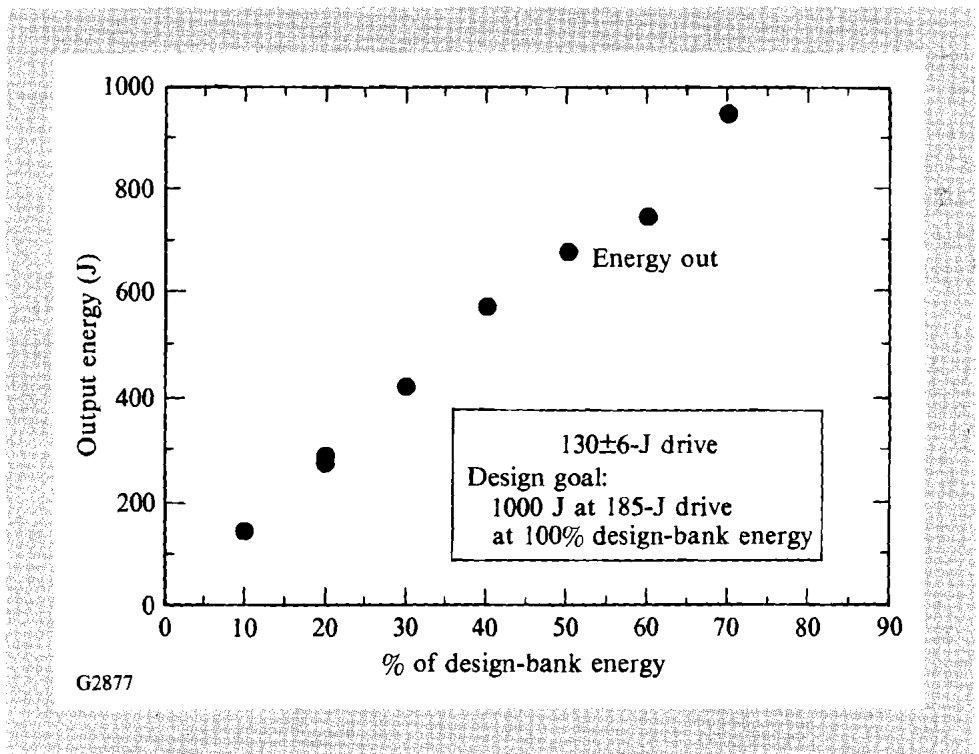


Fig. 44.18

MSA energy output plotted versus percent of the design-bank energy. The MSA achieved 950-J output with 130-J drive at only 70% of the design-bank energy. The design goal was 1000-J output with 185-J drive at 100% of design-bank energy.

#### ACKNOWLEDGMENT

This work was supported by the U.S. Department of Energy Division of Inertial Fusion under agreement No. DE-FC03-85DP40200.

#### REFERENCES

1. LLE Review **41**, 4 (1989).
2. Lawrence Livermore National Laboratory, Laboratory Inertial Confinement Fusion Program, Precision NOVA and NOVA Upgrade Laser, NOVA Upgrade Campaign, Book 2 (1990).
3. Laser Program Annual Report 1985, Lawrence Livermore National Laboratory, UCRL 50021-85 (1986), pp. 7-18-7-24.
4. L. M. Frantz and J. S. Nodvik, *J. Appl. Phys.* **34**, 2346 (1963).
5. Tektronix Inc., Beaverton, Oregon, USA.
6. R. B. Blackman and J. W. Tukey, *The Measurement of Power Spectra* (Dover Publishing, New York, 1958).
7. OMEGA Upgrade Preliminary Design Document, DOE/DP40200-101, p. 9.17 (1989).
8. A. C. Erlandson, H. T. Powell, and R. W. McCracken, Lawrence Livermore National Laboratory, UCRL-ID-104157 (1990).